The A3 adenosine receptor agonist, namodenoson, ameliorates non-alcoholic steatohepatitis in mice

PNINA FISHMAN[1], SHIRA COHEN[1], INBAL ITZHAK[1], JOHNNY AMER[2],
AHMAD SALHAB[2], FAINA BARER[1] and RIFAAT SAFADI[2]

[1]Can-Fite BioPharma Ltd., Petach-Tikva 4951778; [2]Liver Unit, Hadassah University Hospital, Jerusalem 54915, Israel

Abstract. The Wnt/β-catenin pathway confers a chain of molecular events in livers affected by non-alcoholic steatohepatitis (NASH). Namodenoson, a selective agonist of the A3 adenosine receptor (A3AR), which is highly expressed in pathological liver cells, induces a robust anti-inflammatory effect in the liver, mediated via the de-regulation of the Wnt/β-catenin pathway. Namodenoson also acts as a liver protective agent by inhibiting ischemia/reperfusion injury. Based on these unique characteristics, we investigated the anti-NASH effect of Namodenoson in murine models of steatohepatitis and in the LX2 human hepatic stellate cell line (HSC). In the STAM model, Namodenoson significantly decreased the non-alcoholic fatty liver disease (NAFLD) activity score, NAS, demonstrating anti-inflammatory and anti-steatotic effects. In the carbon tetrachloride (CCl4) model, Namodenoson reversed alanine aminotransferase (ALT) to normal values and significantly improved liver inflammation and fibrosis, as well as the adiponectin and leptin levels. Namodenoson de-regulated the Wnt/β-catenin pathway in the liver extracts of the CCl4 model mice and in the LX2 HSCs, manifested by a decrease in the expression of phosphoinositide 3-kinase (PI3K), nuclear factor κ-light-chain-enhancer of activated B cells (NF-κB), β-catenin, lymphoid enhancer-binding factor 1 (Lef-1) and cyclin D1, and an increase in the expression level of glycogen synthase kinase 3β (GSK-3β). The fibrosis marker, α-smooth muscle actin (α-SMA) was also de-regulated, supporting the anti-fibrotic effect of Namodenoson. On the whole, the findings of this study demonstrate that Namodenoson exerts an anti-NASH effect mediated via the de-regulation of the PI3K/NF-κB/Wnt/β-catenin signaling pathway. Thus, targeting A3AR may prove to be a novel direction in the pharmacotherapy of NAFLD/NASH.

Introduction

Non-alcoholic fatty liver disease (NAFLD) is a condition in which fat accumulates in the livers of patients without a history of alcohol consumption (1). The disease occurs in close association with obesity, visceral adiposity, type 2 diabetes and the spectrum of metabolic syndrome (2).

The more advanced form of the disease is designated as non-alcoholic steatohepatitis (NASH) and manifests, apart from steatosis, as intra-lobular inflammation, hepatocellular ballooning and progressive fibrosis (3). Long-lasting NASH may progress to liver cirrhosis and hepatocellular carcinoma (HCC) (4). The higher incidence of co-morbidity risk factors in patients with NASH-derived HCC leads to a lower overall survival compared to patients with HCC which has developed due to other etiologies. Over the past decades, the prevalence of NAFLD/NASH has markedly increased, more than doubling from 1999-2002 to 2009-2012. Among the westernized countries, 20% of the general adult population presents with hepatic steatosis, with 2-3% suffering from NASH (2).

Due to the multifactorial nature of NAFLD/NASH, a variety of drug candidates aiming at different molecular targets, involved with disease etiology and pathogenesis, have been tested to reverse or ameliorate the disease. These include insulin sensitizers (such as thiazolidinediones and metformin); hepatoprotective agents, including those with antioxidant properties (such as ursodeoxycholic acid and vitamin E); bile acid analogues (such as obeticholic acid), metabolically active agents (such as weight loss drugs and hypouricemic agents); and drugs that affect fat metabolism (such as statins and other hypolipidemic agents, fibrates, acetyl-CoA carboxylase inhibitors and aramchol) (5-7). More drug candidates which target specific molecular pathways,

such as the peroxisome proliferator-activated receptor (PPAR), farnesoid X receptor (FXR), glucagon-like peptide-1 and thyroid hormone receptor β (TRβ), are under development; however, to date, to the best of our knowledge, the US FDA has not approved any drug for the specific treatment of NAFLD/NASH (8).

Namodenoson is a synthetic adenosine derivative that binds with high selectivity to the A3 adenosine receptor (A3AR) in pathological liver cells, inducing robust anti-inflammatory and anti-cancer effects. It has been well established that extracellular adenosine signaling is mediated via 4 receptors: A_1, A_{2A}, A_{2B} and A_3. The latter has the lowest affinity to adenosine and is overexpressed in liver cells derived from inflammatory and tumor tissues, whereas a low expression is found in normal liver cells (9-11).

It has been well documented that A3AR is upregulated in tumor and inflammatory liver tissues compared to normal liver cells, suggesting a role for A3AR in human liver diseases (9). Selective agonists which bind to the A3AR with high affinity induce a marked anti-inflammatory and anti-cancer effect in experimental animal models of autoimmune hepatitis and in orthotopic and xenograft liver cancer models (9,10).

Data from a phase I/II trial in patients with advanced HCC treated with Namodenoson demonstrated anti-tumor activity and the prolongation of the overall survival time with an excellent safety profile (12). The molecular mechanisms of action involved with the anti-inflammatory and anticancer effects of A3AR agonists, entail inhibition of cyclic adenosine monophosphate (c-AMP), protein kinase A (PKA), phosphoinositide 3-kinase (PI3K) and p-Akt (9,13,14). These effects give rise to the de-regulation of the nuclear factor κ-light-chain-enhancer of activated B cells (NF-κB) and the Wnt/β-catenin pathways, known to mediate anti-inflammatory, anti-steatotic, anti-fibrotic and anticancer effects (9,15-17).

Of note, Namodenoson also acts as a protective agent against liver damage in ischemia and partial hepatectomy. It has been found to exert a protective effect on normal liver tissues in an experimental model of liver inflammation (9,11), suggesting its use as a therapeutic agent in subjects with hepatic impairment. Taken together, these findings suggest a differential effect of Namodenoson on pathological cells manifested via its anti-inflammatory/anticancer effect, and at the same time, a hepatoprotective effect towards normal liver cells.

Based on the unique characteristics of Namodenoson, in this study, we aimed to determine the utility of the drug in 3 experimental models of NAFLD/NASH disease. The findings of this study demonstrate that Namodenoson exhibits a triple-mechanism of action in the liver, exerting anti-steatotic, anti-inflammatory and anti-fibrotic effects. The upstream targeting of these pathways is likely an effective and symbiotic combination for a promising candidate for the treatment of NASH.

Materials and methods

Reagents. The A3AR agonist, Namodenoson, is a compound known generically as 2-chloro-N6-(3-iodobenzyl)-adenosine-5'-N-methyl-uronamide, was synthesized for Can-Fite BioPharma by Albany Molecular Research Inc. A stock solution of 5.44 mg/ml was prepared in DMSO and further diluted in PBS for the *in vivo* and *in vitro* experiments.

STAM mouse model. C57BL/6 mice (14-day-pregnant, female) were obtained from Japan SLC, Inc. All animals used in this study were housed and cared for in accordance with the Japanese Pharmacological Society Guidelines for Animal Use. The animals were maintained in a SPF facility under controlled conditions of temperature (23±2˚C), humidity (45±10%), lighting (12-h artificial light and dark cycle; light from 08:00 to 20:00) and air exchange. A high pressure was maintained in the experimental room to prevent the contamination of the facility. The animals were housed in TPX cages (CLEA Japan, Inc.) with a maximum of 4 mice per cage. Sterilized Paper-Clean (Japan SLC) was used for bedding and was replaced once a week. A sterilized solid high-fat diet (HFD) was provided *ad libitum*. NASH was induced in 24 male mice by a single subcutaneous injection of 200 µg streptozotocin (STZ, Sigma-Aldrich Co. LLC.) solution 2 days after birth. At 4 weeks of age, feeding with a HFD (57 kcal% fat, cat. no. HFD32, CLEA Japan, Inc.) was initiated till sacrifice. Namodenoson at 200 µg/kg (n=8) or equal amounts of DMSO (n=16) treatments were administered p.o., thrice daily between weeks 6-9.

Mouse model of carbon tetrachloride (CCl4)-induced liver fibrosis. Eleven-week-old male C57bl/6J male mice (n=21), from Harlan Laboratories, and housed in a barrier facility and received care according to the NIH guidelines. All procedures involving laboratory animals were evaluated and approved by The Hebrew University Institutional Animal Care and Use Committee and followed the guidelines for laboratory animal welfare.

The mice (n=16) received an intraperitoneal (i.p.) injection of CCl4 at 0.5 ml/kg body weight (1:10 v/v in corn oil) (Sigma). Namodenoson at the dose of 100 µg/kg body was administered by i.p. injection twice a week, commencing one day after the first dose of CCl4 (n=8) or the vehicle (n=8) (corn oil) twice a week for 6 weeks, as previously described (18). In addition, 5 naïve mice with no treatments have been included as well. The mice were sacrificed at 72 h after the final CCl4 injection. Whole livers and serum were collected for histological, cytological, biochemical and molecular analyses.

The animals of both models were sacrificed by exsanguination through direct cardiac puncture under ether anesthesia.

Serum alanine aminotransferase (ALT) measurement. Blood samples were collected from C57bl/6J male mouse hearts at a volume of 0.5 ml. The samples were centrifuged for 5 min at 3,584 x g, at 4˚C, and the supernatants (volume of 600 µl) were transferred to Eppendorf tubes. Serum samples of 32 µl were dropped onto the strip of the ALT (Reflotron) and analyzed by Reflovet® plus (Roche).

Histopathological analyses. Livers from the STAM and CCl4 model mice were harvested and fixed in 4% formaldehyde for 48 h. Paraffin slides of 3-5 µ thickness were stained as described below. The evaluation of the slides was performed using a microscope (Olympus BX60, serial no. 7D04032 at a magnification of x10) and microscope Camera (Olympus DP73, serial no. OH05504). Ten random fields were observed for each slide. For the STAM model slides, hematoxylin and eosin (H&E) staining was used to analyze inflammation,

steatosis and ballooning, combined as the NAFLD activity score (NAS) and calculated according to the Kleiner criteria (19) (Table I). To assess the adiponectin quantity, immunofluorescence mouse anti-adiponectin (1:50, cat. no. ab22554, Abcam) was used. The stained sections were examined under a fluorescence microscope (E600, Nikon) equipped with a Plan Fluor objective connected to a CCD camera (DMX1200F, Nikon). Digital images were collected and analyzed using Image-Pro Plus software 6.3. Images were assembled using Adobe Photoshop (Adobe Systems). In addition, immunohistological analysis utilizing rabbit anti-adiponectin/Acrp30 antibody (cat. no. NB100-6581; Novus Biologicals) at a dilution of 1:10 was performed to reproduce images. For the CCl4 model slides, the following analyses were performed: i) Sirius Red staining for fibrosis assessment; and ii) immunohistological analysis utilizing rabbit anti-adiponectin/Acrp30 antibody and rabbit anti leptin/OB antibody (cat. no. NBP1-59324; Novus Biologicals) at a 1:10 dilution, respectively, for the assessment of adiponectin and leptin.

Inflammation assessment (H&E staining). For the assessment of inflammation, H&E staining was carried out. The sections were graded as follows: Grade 0, no inflammation; grade 1, mild/few inflammatory cells, 10-20 per X20 high-power field (HPF); grade 2, moderate/more inflammatory cells, 20-50 per X20 HPF; and grade 3, severe/many inflammatory cells, >50 per X20 HPF.

Fibrosis assessment (Sirius Red staining). The liver sections were stained with Picro-Sirius Red solution (Waldeck). Morphometric analysis was performed using 'Image Pro Plus; version 6.3 (Media Cybernetics)'.

Adiponectin and leptin assessment. For adiponectin and leptin assessment, the sections were graded as follows: Grade 0, no positive reaction of IHC at all; grade 1, only few cells are immunopositive to the stain (<5 cells per a x10 field); grade 2, very mild immune reaction (>5 and <15 cells per a x10 field); grade 3, mild immune reaction (>15 and <25 cells per a x10 field); grade 4, moderate immune reaction (>25 and <50 cells per a x10 field); and grade 5, high immune reaction (>50 cells per a x10 field).

RT-qPCR. Total cellular RNA was isolated from liver tissue, using 2 ml TRI Reagent (Bio LAB; Jerusalem, Israel) for each 3 cm of tissue. The samples were homogenized for 5 min at room temperature of 25°C. 0.2 ml of Chloroform (Bio LAB; Jerusalem, Israel) were added to each sample, incubated for 15 min at room temperature and centrifuged (1,400 rpm) for 15 min at 4°C. The supernatant in each sample was transferred to new Eppendorf, 0.5 ml of isopropanol (Bio-Lab Ltd.) were added to the sample for 10 min at 25°C and centrifuged (32,256 x g) for 10 min at 4°C. The supernatants were removed and 1 ml of 75% ethanol was added to the pellet and centrifuged (12,600 x g) for 5 min at 4°C. The pellets were dried in air at room temperature for 15 min, 50 μl of DEPC were added, and the samples were heated for 10 min at 55°C. The preparation of cDNA was performed using High Capacity cDNA Isolation kit (R&D Systems). RT-qPCR was performed for the quantification of the expression of the gene that encoded α-SMA (Rhenium

Table I. NAS calculation by Kleiner criteria.

Item	Score	Extent
Steatosis	0	<5%
	1	5-33%
	2	>33-66%
	3	>66%
Hepatocyte ballooning	0	None
	1	Few balloon cells
	2	Many cells/prominent ballooning
Lobular inflammation	0	No foci
	1	<2 foci/200x
	2	2-4 foci/200x
	3	>4 foci/200x

NAS, non-alcoholic fatty liver disease (NAFLD) activity score.

Assay ID: Mm00725412s1), compared to GAPDH (Rhenium Assay ID: Mm99999915g1) as a housekeeping gene using TaqMan Fast Advanced Master Mix (Applied Biosystems). Relative gene expression data were analyzed using the $2^{-\Delta\Delta Cq}$ method (20).

Semi-quantitative PCR. For the LX2 cells, total RNA was extracted using TRI-Reagent (Sigma). RNA (500 ng) was reverse transcribed using the high-capacity cDNA reverse transcription kit (Thermo Fisher Scientific) according to the manufacturer's instructions. RT-qPCR was performed for the quantification gene expression of the encoded α-SMA, compared to β-actin as a housekeeping gene using TaqMan Fast Advanced Master Mix (Applied Biosystems). For α-SMA, the primers forward. 5'-ACTGGGACGACATGGAAAAG-3' and reverse. 5'-TACATGGCTGGGACATTGAA-3' were added. The PCR reaction was performed as follows: Heating to 94°C for 2 min, 25 cycles of 94°C for 15 sec, 56°C for 45 sec, and 68°C for 2 min. For the amplification of human β-actin, the primers forward. 5'-TGGGAATGGGTCAGAAGGACT-3' and reverse. 5'-TTTCACGGTTGGCCTTAGGGT-3' were used. The PCR condition included heating to 94°C for 2 min, 25 cycles of 94°C for 30 sec, 56°C for 1 min and 30 sec, and 72°C for 45 sec. The PCR products were electrophoresed on 2% agarose gels, stained with ethidium bromide and visualized with UV illumination. Total Lab v1.11 software was used for quantification.

Cell culture. LX2 human hepatic stellate cells (HSCs; ATCC) were grown in DMEM containing penicillin (10 units/ml), streptomycin (10 μg/ml), L-glutamine (2 mM) and 10% fetal bovine serum (FBS). The cells were maintained in T-75 flasks at 37°C in a 5% CO_2 incubator and transferred to a freshly prepared medium twice weekly. For all experiments, serum-starved cells were used. FBS was omitted from the cultures for 18 h and the experiment was carried out on monolayers of cells in DMEM supplemented with 1% FBS in a 37°C, 5% in a CO_2 incubator.

³H-thymidine incorporation assay. ³H-thymidine incorporation assay was used to evaluate cell growth. LX2 cells (5,000 cells/well) were incubated (37°C) with 10 nM Namodenoson in the absence or presence of the antagonist, MRS 1523 (5 nM) (cat. no. M1809; Sigma-Aldrich), in a 96-well plate for 48 h. Each well was pulsed with 1 μ Ci ³H-thymidine for the last 24 h. The cells were harvested and the ³H-thymidine uptake was determined in an LKB liquid scintillation counter (LKB). These experiments were repeated at least 4 times.

Western blot analysis. Protein extracts from liver tissue or the LX-2 cell line were utilized. The liver tissue was homogenized with an ice-cold RIPA lysis buffer (Sigma) with protease phosphatase inhibitor cocktail (Roche). The LX2 cells were rinsed with ice-cold PBS and transferred to ice-cold lysis buffer (TNN buffer, 50 mM Tris buffer pH 7.5, 150 mM NaCl, NP 40 0.5% for 20 min). Cell debris was removed by centrifugation for 10 min, at 7,500 x g, 4°C. The supernatant was utilized for western blot analysis. Protein concentrations were determined using the NanoDrop spectrophotometer (Thermo Fisher Scientific). Equal amounts of the sample (50 μg) were separated by SDS-PAGE, using 4-12% polyacrylamide gels. The resolved proteins were then electroblotted onto nitrocellulose membranes (Pall Corp.). The membranes were then blocked with 5% bovine serum albumin and incubated with the desired primary antibody [A3AR, sc-13938; PI3K, sc-1637; glycogen synthase kinase 3β (GSK-3β), sc-9166; β-catenin, sc-7963; cyclin D1, sc-8396; NF-κB, sc-372; lymphoid enhancer-binding factor 1 (LEF-1), sc-374522; α-SMA, sc-32251; and β-actin, sc-47778; dilution 1:1,000; all from Santa Cruz Biotechnology] for 24 h at 4°C. The blots were then washed and incubated with a secondary antibody (Abcam; mouse ab97020, rabbit ab97048) for 1 h at room temperature. Bands were recorded using the BCIP/NBT color development kit (Promega). Densitometry of protein expression was normalized against β-actin and expressed as a percentage of the control.

Statistical analysis. Statistical analyses for the comparison between 2 groups were performed using the Student's t-test. Significant differences between multiple groups were determined using one-way ANOVA followed by Tukey's post-hoc analysis. P-values <0.05 were considered to indicate statistically significant differences. Data are presented as the means ± SD. The Chi-squared test was used for the assessment of ascites. For both analyses, P-values <0.05 were considered indicate statistically significant differences.

Results

Namodenoson improves NAS in the STAM model. A representative photomicrograph of H&E-stained liver sections is depicted in Fig. 1A, demonstrating that in the vehicle-treated group, inflammatory cell infiltration, severe micro- and macrovesicular fat deposition and hepatocellular ballooning had occurred. Namodenoson treatment between weeks 6 to 9 resulted in a significant reduction in steatosis and an improvement in inflammation and ballooning, as demonstrated by morphometric analysis (P<0.05, P<0.05 and P<0.01,

respectively), summing up to a significant decrease in the NAS score compared to the vehicle-treated group (Fig. 1B). Moreover, intense adiponectin staining was observed in liver sections derived from the Namodenoson-treated group compared to the vehicle treated one (Fig. 1C, left panel) and quantification is depicted in the right panel of Fig. 1C, utilizing immunofluorescence antibody (P<0.01).

Anti-NAFLD/NASH effects of Namodenoson in the CCl4 model. In the CCl4 model, the serum ALT levels increased from 63.65±2.36 to 294.75±69.24 (P<0.01). Namodenoson significantly decreased the serum ALT levels, returning them to near normal levels (69.35±17.64; P<0.01; Fig. 2A). Namodenoson also reversed the ascites induced by CCl4 compared to the vehicle-treated group (P<0.05; Fig. 2B). Morphometric analysis of the liver sections derived from the CCL4-treated mice revealed an upregulation of inflammation, fibrosis, adiponectin and leptin, whereas a significant reduction was noted in the samples derived from the Namodenoson-treated mice (P<0.01; Fig. 2C).

Western blot analysis of the liver extracts derived from the animals in the CCl4 model revealed that Namodenoson treatment induced a decrease in the A3AR and PI3K expression levels followed by an increase in the GSK-3β expression level, with a subsequent reduction in the levels of β-catenin and cyclin D1, key proteins of the Wnt signaling pathway (Fig. 2D). The mRNA expression level of α-SMA was markedly decreased in the Namodenoson-treated group compared with the vehicle-treated group (P<0.01; Fig. 2E).

Namodenoson inhibits LX2 cell Proliferation and modulates key growth regulatory proteins. Namodenoson inhibited LX2 cell proliferation as was measured by ³H-thymidine incorporation. The highly specific A3AR antagonist, MRS 1523, counteracted the inhibitory effect of Namodenoson (P<0.01; Fig. 3A). Western blot analysis revealed that upstream, Namodenoson treatment induced the downregulation of A3AR, PI3K, NF-κB and α-SMA expression; these effects were reversed by MRS 1523, demonstrating the specificity of the response to the agonist (Fig. 3B). Downstream, GSK-3β was up-regulated whereas β-catenin, Lef-1 and cyclin D1 were down-regulated (Fig. 3C). Moreover, a decrease in α-SMA mRNA expression was noted (Fig. 3D). As can been seen, the protein profile was very similar to that of the liver extracts derived from the Namodenoson-treated CCL4 animals, supporting the notion that Namodenoson deregulates the Wnt/β-catenin pathway.

Discussion

In this study, we demonstrate that the A3AR agonist, Namodenoson, exerts significant anti-inflammatory, anti-steatotic and anti-fibrotic effects on the STAM and the CCl4 animal models, as well as on human LX2 HSCs. Namodenoson is an agonist at the Gi protein-associated A3AR, and is overexpressed in inflammatory and cancer cells; however, its expression is very low even absent in normal body cells (9,13). It has been previously demonstrated by us and others that A3AR activation with a specific agonist induces the apoptosis of both inflammatory and cancer cells, whereas normal cells
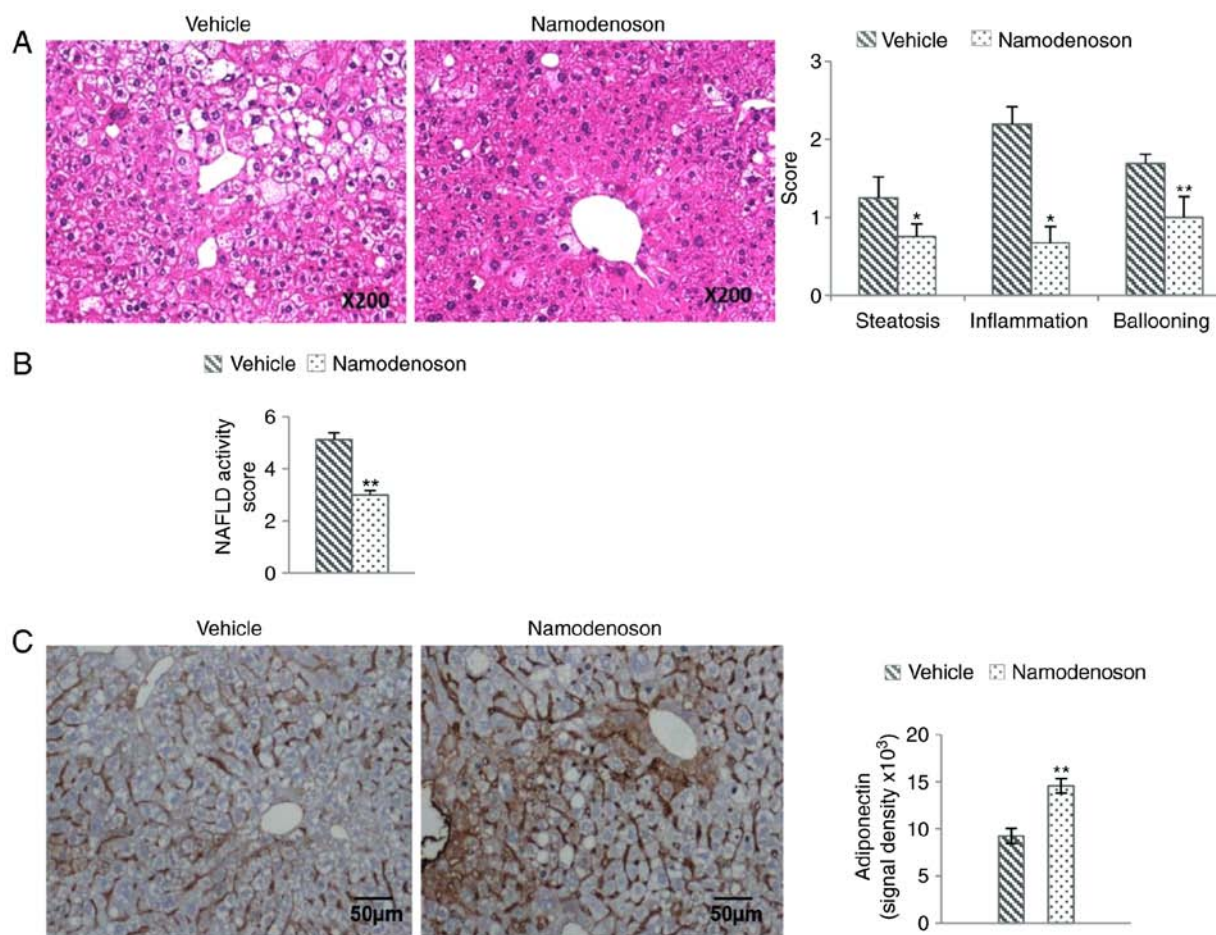
Figure 1. Namodenoson reduces NAS and elevates adiponectin in the STAM model. Streptozotocin-injected mice were fed a high-fat diet and Namodenoson or the vehicle (DMSO) were administered p.o. thrice daily (200 μg/kg) during weeks 6-9. (A) Representative liver sections of H&E staining demonstrating an improvement in steatosis, inflammation and ballooning in the Namodenoson-treated group vs. the vehicle. (B) Effects of Namodenoson on NAS. (C) Immunohistochemical staining depicting an increase in adiponectin upon Namodenoson treatment. The data represent the means ± SEM. Statistical analysis was carried out using a two-tailed Student's t-test. *P<0.05, **P<0.01, Namodenoson vs. vehicle; n=8-14 animals/group. [Hematoxylin and eosin (H&E) staining: Original magnification, x100]; adiponectin staining: Original magnification, x40. NAS, non-alcoholic fatty liver disease (NAFLD) activity score.

are refractory to the effect of the agonist. The effect towards the pathological cells was mediated via the deregulation of both the NF-κB and the Wnt/β-catenin signaling pathways and led to the inhibition of inflammatory cytokine production, resulting in the apoptosis of inflammatory and cancer cells (10,13,21).

These unique characteristics of the A3AR agonists served as the rational to try and utilize Namodenoson as an anti-NAFLD/NASH agent. Indeed, in the STAM model, a decrease in steatosis, lobular inflammation and ballooning was recorded, altogether yielding a significant reduction in NAS, pointing towards the anti-NAFLD/NASH effects of Namodenoson. In the CCl4 model, Namodenoson also induced a robust anti-inflammatory effect manifested by its capability to reverse the H&E inflammation morphometric score and ALT serum levels to normal values. Similar data were previously observed in a mouse model of Concanavalin A-induced hepatitis upon treatment with A3AR ligands, which reversed the increase in liver enzymes to normal values and inhibited inflammatory cytokine production and additional manifestations of liver inflammation (10,21).

In the current study, a decrease in NF-κB expression levels, both *ex vivo* in the CCl4 model, and in the LX-2 hepatic stellate cells *in vitro*, supports the anti-inflammatory effects of Namodenoson. Moreover, morphometric analysis of adiponectin, usually negatively associated with parameters of the metabolic syndrome, revealed a significant increase in adiponectin staining in the Namodenoson-treated mice, supporting the anti-inflammatory and anti-metabolic effects of the drug. Of note, adiponectin is known to be overexpressed in the CCl4 model (22) and in the current study Namodenoson treatment reversed the adiponectin levels to those of the naïve mice, demonstrating its beneficial effect.

The following molecular chain of events took place both in the liver extracts derived from the CCl4 model and in the LX-2 HSCs. Upstream, the downregulation of A3AR and PI3K occurred immediately following treatment with Namodenoson, followed by a decrease in the expression levels of NF-κB and α-SMA. The response was highly specific to Namodenoson treatment since the introduction of an antagonist (MRS 1523), to the LX-2 cell cultures, reversed the decrease in the levels of A3AR, PI3K, NF-κB and α-SMA. A3AR downregulation upon treatment with a specific agonist has been previously described and is a result of receptor internalization and degradation in the cytoplasm. The receptor is then re-synthesized and re-cycle to the cell surface (23).
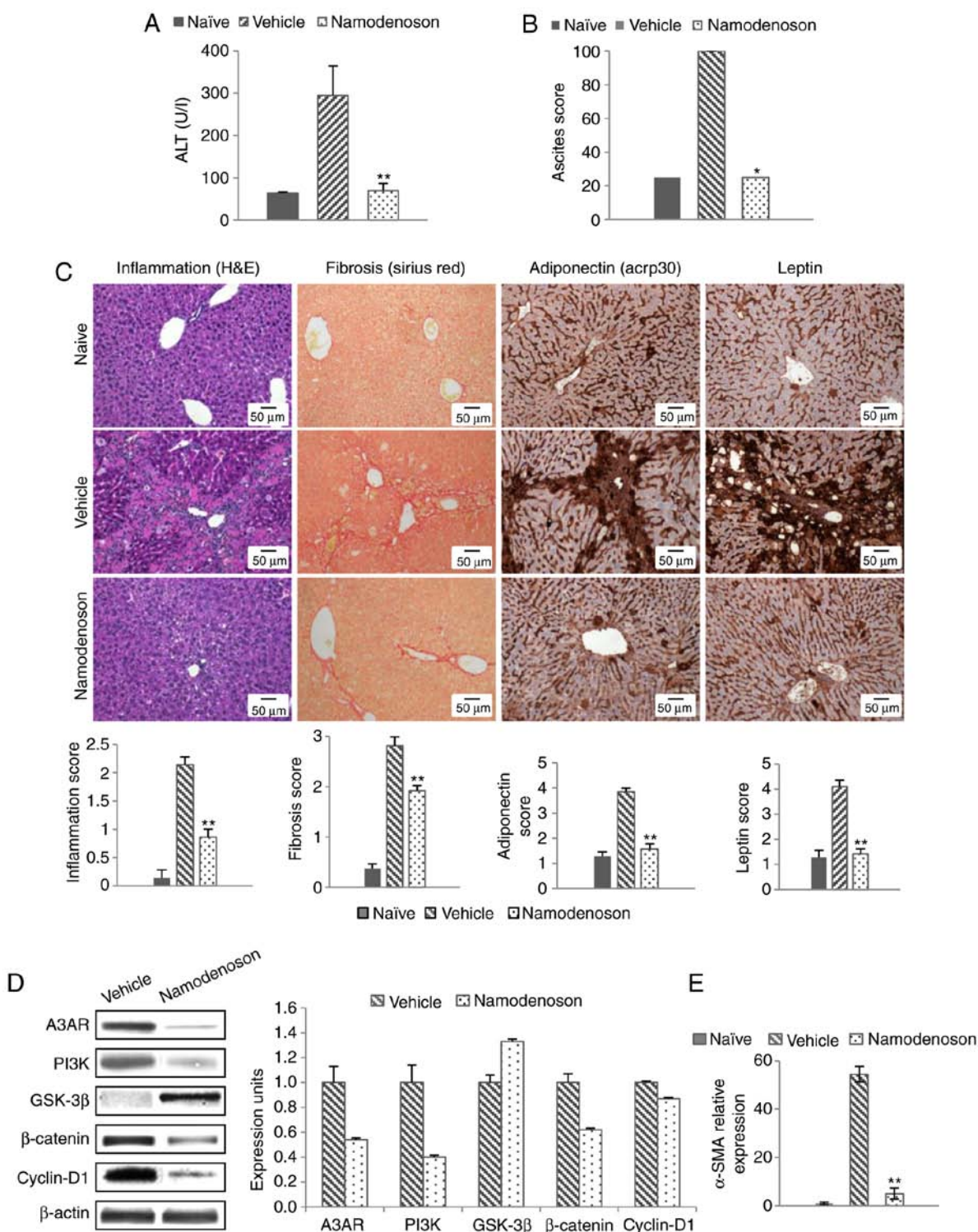
Figure 2. Namodenoson ameliorates liver functions and pathology via the deregulation of the Wnt/β-catenin pathway in the CCl4 model. CCL4-injected mice were treated twice weekly via i.p. injection with Namodenoson (100 μg/kg) or the vehicle (DMSO). The levels of (A) serum ALT and (B) ascites were reversed to those of the naïve group following treatment with Namodenoson. (C) Representative stained liver sections demonstrating an improvement in inflammation (H&E staining), fibrosis (Sirius Red staining), adiponectin and leptin (immunohistochemistry); original magnification, x40 (D) Representative western blots of the protein expression of A3AR, PI3K, GSK-3β, β-catenin and cyclin-D1 in mouse liver extracts. β-Actin served as an internal control. (E) mRNA expression of α-SMA. The data represent the means ± SEM. Statistical analysis was carried out by one-way ANOVA followed by Tukey's post-hoc analysis in panels A, C and E. The Chi-squared test was used for ascite assessment in panel B; *P<0.05, **P<0.01, vehicle vs. naïve and Namodenoson vs. vehicle; n=8 animals/group. A3AR, A3 adenosine receptor; PI3K, phosphoinositide 3-kinase; GSK-3β, glycogen synthase kinase 3β; α-SMA, α-smooth muscle actin.

A plethora of mechanistic pathways occur downstream to PI3K deregulation and play a role in mediating the effects of Namodenoson recorded in the present study. Both the Wnt/β-catenin and the NF-κB pathways are controlled upstream by PI3K and were deregulated upon treatment with Namodenoson. Moreover, the Wnt/β-catenin pathway is also known to be involved in the pathogenesis of fibrosis and steatosis in hepatic stellate cells (15,24,25). In the CCl4 liver extracts and
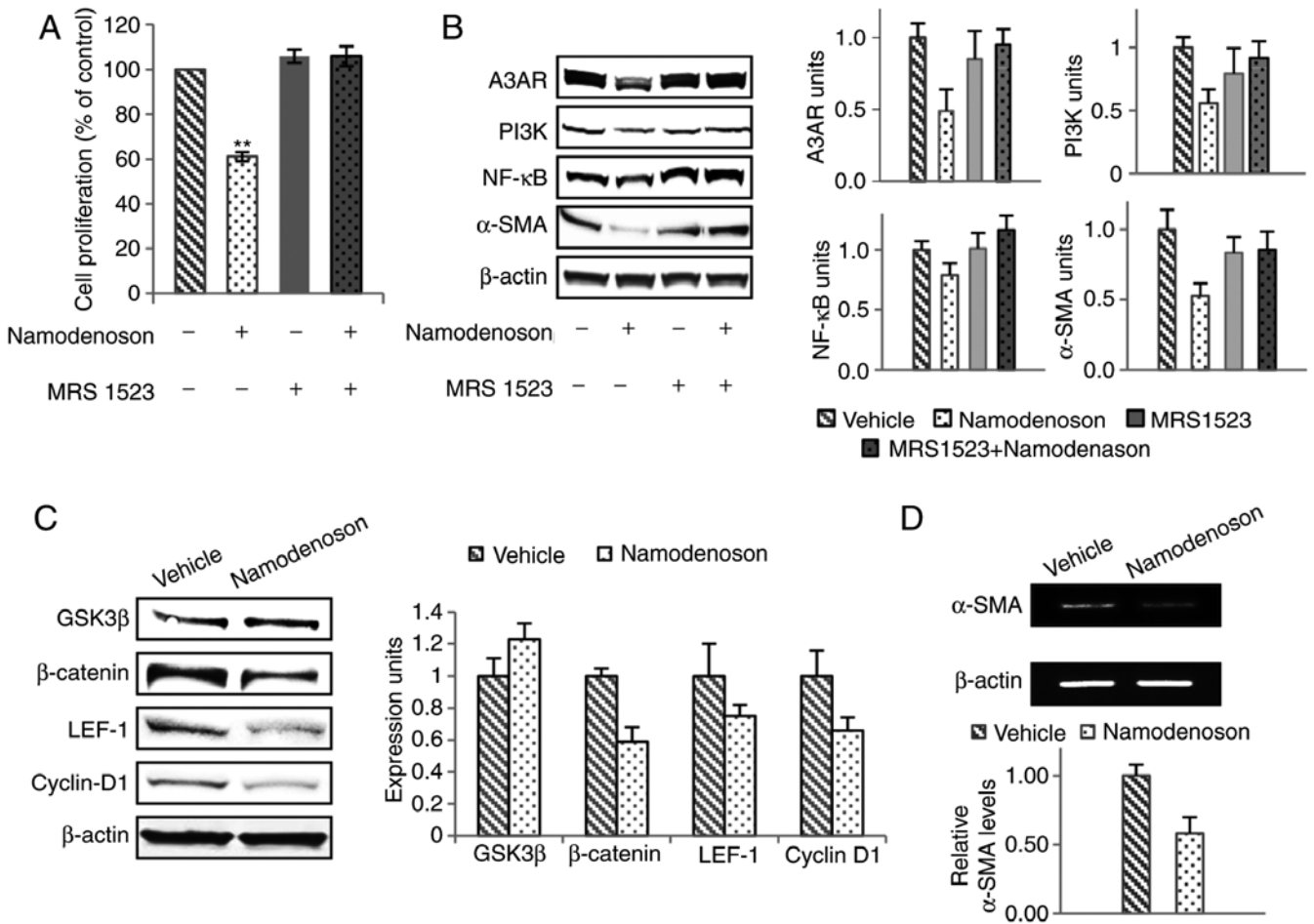
Figure 3. Namodenoson induces the proliferation inhibition and modulation of cell growth regulatory proteins in LX-2 HSCs. Cells were incubated for 48 h with the vehicle, Namodenoson (10 nM), the A3AR antagonist, MRS 1523 (5 nM), and a combination of the agonist and the antagonist. (A) Cell proliferation. The data represent the means ± SEM. Statistical analysis was carried out by one-way ANOVA followed by Tukey's post-hoc analysis. **P<0.01, vehicle vs. Namodenoson; 4 independent experiments. (B) Western blot analyses of A3AR, PI3K, NF-κB and α-SMA. (C) Western blot analyses of β-catenin, GSK-3β, LEF-1 and cyclin D1; β-actin was used as a loading control. (D) α-SMA mRNA expression examined by RT-qPCR. A3AR, A3 adenosine receptor; PI3K, phosphoinositide 3-kinase; GSK-3β, glycogen synthase kinase 3β; LEF-1, lymphoid enhancer-binding factor 1; α-SMA, α-smooth muscle actin.

the LX2 HSCs, GSK-3β was found to be upregulated with a subsequent decrease in the expression levels of β-catenin, Lef-1 and cyclin D1, the latter being responsible for proliferation of HSCs in the liver and also essential for the evolution of liver fibrosis and steatosis (26). Additional support for the anti-fibrotic effect of Namodenoson came from its ability to decrease mRNA and protein expression levels of α-SMA, known directly to be controlled by PI3K, and serve as biomarker for fibrosis (16). A decrease in PI3K most probably led to a subsequent decrease in α-SMA, contributing to the anti-fibrotic effect of Namodenoson. Moreover, adiponectin directly inhibits the activation of HSCs, thereby playing a role in the prevention of fibrosis (27).

It thus seems that the Wnt/β-catenin pathway acts as the 'policeman' at the crossroads of steatosis, inflammation and fibrosis. A cartoon summarizing the molecular events taking place in pathological liver cells upon treatment with Namodenoson is presented in Fig. 4.

A side benefit of Namodenoson can be the cardio-protective and neuro-protective characteristic of the drug, extensively published over the past decade and may compensate for the cardiovascular and diabetic diseases which are part of the pathogenesis of NAFLD/NASH (28,29).
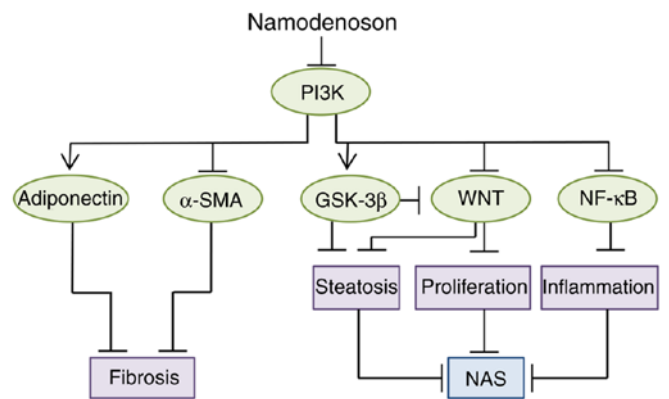

Figure 4. Proposed mechanism confers the anti-NASH effect of Namodenoson in the liver. Namodenoson via A3AR, downregulates the key protein PI3K, deregulates the NF-κB and the WNT signaling pathways, as well as α-SMA, leading to the inhibition of proliferation, inflammation, steatosis and fibrosis. The latter is also inhibited by adiponectin which is upregulated upon the inhibition of PI3K. The GSK3-β expression level is also increased, affecting as well the decrease of steatosis, altogether resulting in NAS inhibition. A3AR, A3 adenosine receptor; PI3K, phosphoinositide 3-kinase; GSK-3β, glycogen synthase kinase 3β; LEF-1, lymphoid enhancer-binding factor 1; α-SMA, α-smooth muscle actin; NAS, non-alcoholic fatty liver disease (NAFLD) activity score.

Taken together, this study demonstrates that Namodenoson exhibits a triple-mechanism of action in the liver, exerting anti-steatosis, anti-inflammatory and anti-fibrotic effects through the activation of the A3AR and deregulation of the NF-κB and the Wnt/β-catenin pathways. Thus, the upstream targeting of these pathways is likely an effective and symbiotic combination for a promising candidate for the treatment of NASH.

Acknowledgements

Funding

Availability of data and materials

We confirm that the compound described in the manuscript is in the purity of 99.9%. the source is Albany Molecular Research Inc USA. All data generated or analyzed during this study are included in this published article or are available from the corresponding author on reasonable request.

Authors' contributions

PF, RS and SC developed the study concept and designed the study. SC, II, FB, JA and AS performed the experiments and procedures. PF, SC and II wrote the manuscript. All authors have read and approved the final manuscript.

Ethics approval and consent to participate

All procedures involving laboratory animals were evaluated and approved by The Hebrew University Institutional Animal Care and Use Committee and followed the guidelines for laboratory animal welfare.

Patient consent for publication

Not applicable.

Competing interests

The authors with potential competing interests are detailed as follows: PF is an employment and stock options holder; SC is a consultant and stock options holder; FB is an employment and stock options holder; II is an employment and RS a stock options holder. The authors with no competing interests are detailed as follows: JA and AS.

References

1. Ratziu V, Bellentanib S, Cortez-Pintoc H, Dayd C and Marchesinie G: A position statement on NAFLD/NASH based on the EASL 2009, special conference. J Hepatol 53: 372-384, 2010.
2. Williams CD, Stengel J, Asike MI, Torres DM, Shaw J, Contreras M, Landt CL and Harrison SA: Prevalence of nonalcoholic fatty liver disease and nonalcoholic steatohepatitis among a largely middle-aged population utilizing ultrasound and liver biopsy: A prospective study. Gastroenterology 140: 124-131, 2011.
3. Chalasani N, Younossi Z, Lavine JE, Diehl AM, Brunt EM, Cusi K, Charlton M and Sanyal AJ: The diagnosis and management of non-alcoholic fatty liver disease: Practice guideline by the American association for the study of liver diseases, American college of gastroenterology, and the American gastroenterological association. Hepatology 55: 2005-2023, 2012.
4. Dhamija E, Paul SB and Kedia S: Non-alcoholic fatty liver disease associated with hepatocellular carcinoma: An increasing concern. Indian J Med Res 149: 9-17, 2019.
5. Ratziu V, Goodman Z and Sanyal A: Current efforts and trends in the treatment of NASH. J Hepatol 62 (Suppl 1): S65-S75, 2015.
6. Takahashi Y, Sugimoto K, Inui H and Fukusato T: Current pharmacological therapies for nonalcoholic fatty liver disease/nonalcoholic steatohepatitis. World J Gastroenterol 21: 3777-3785, 2015.
7. Guillaume M and Ratziu V: Pharmacological agents for nonalcoholic steatohepatitis. Hepatol Int 7 (Suppl 2): 833-841, 2013.
8. Cave MC, Clair HB, Hardesty JE, Falkner KC, Feng W, Clark BJ, Sidey J, Shi H, Aqel BA, McClain CJ and Prough RA: Nuclear receptors and nonalcoholic fatty liver disease. Biochim Biophys Acta 1859: 1083-1099, 2016.
9. Bar-Yehuda S, Stemmer SM, Madi L, Castel D, Ochaion A, Cohen S, Barer F, Zabutti A, Perez-Liz G, Del Valle L and Fishman P: The A3 adenosine receptor agonist CF102 induces apoptosis of hepatocellular carcinoma via de-regulation of the Wnt and NF-kappaB signal transduction pathways. Int J Oncol 33: 287-295, 2008.
10. Cohen S, Stemmer SM, Zozulya G, Ochaion A, Patoka R, Barer F, Bar-Yehuda S, Rath-Wolfson L, Jacobson KA and Fishman P: CF102 an A3 adenosine receptor agonist mediates anti-tumor and anti-inflammatory effects in the liver. J Cell Physiol 226: 2438-2447, 2011.
11. Ohana G, Cohen S, Rath-Wolfson L and Fishman P: A3 adenosine receptor agonist, CF102, protects against hepatic ischemia/reperfusion injury following partial hepatectomy. Mol Med Rep 14: 4335-4341, 2016.
12. Stemmer SM, Benjaminov O, Medalia G, Ciuraru NB, Silverman MH, Bar-Yehuda S, Fishman S, Harpaz Z, Farbstein M, Cohen S, et al: CF102 for the treatment of hepatocellular carcinoma: A phase I/II, open-label, dose-escalation study. The Oncologist 18: 25-26, 2013.
13. Ochaion A, Bar-Yehuda S, Cohen S, Amital H, Jacobson KA, Joshi BV, Gao ZG, Barer F, Patoka R, Del Valle L, et al: The A3 adenosine receptor agonist CF502 inhibits the PI3K, PKB/Akt and NF-kappaB signaling pathway in synoviocytes from rheumatoid arthritis patients and in adjuvant-induced arthritis rats. Biochem Pharmacol 76: 482-494, 2008.
14. Fishman P, Bar-Yehuda S, Madi L, Rath-Wolfson L, Ochaion A, Cohen S and Baharav E: The PI3K-NF-κB signal transduction pathway is involved in mediating the anti-inflammatory effect of IB-MECA in adjuvant induced arthritis. Arthritis Res Ther 8: R33, 2006.
15. Miao CG, Yang YY, He X, Huang C, Huang Y, Zhang L, Lv XW, Jin Y and Li J: Wnt signaling in liver fibrosis: Progress, challenges and potential directions. Biochimie 95: 2326-2335, 2013.
16. Zhang C, Liu XQ, Sun HN, Meng XM, Bao YW, Zhang HP, Pan FM and Zhang C: Octreotide attenuates hepatic fibrosis and hepatic stellate cells proliferation and activation by inhibiting Wnt/β-catenin signaling pathway, c-Myc and cyclin D1. Int Immunopharmacol 63: 183-190, 2018.
17. Matsuda S, Kobayashi M and Kitagishi Y: Roles for PI3K/akt/PTEN pathway in cell signaling of nonalcoholic fatty liver disease. ISRN Endocrinol 2013: 472432, 2013.
18. Abu-Tair L, Axelrod JH, Doron S, Ovadya Y, Krizhanovsky V, Galun E, Amer J and Safadi R: Natural killer cell-dependent anti-fibrotic pathway in liver injury via toll-like receptor-9. PLoS One 8: e82571, 2013.
19. Kleiner DE, Brunt EM, Van Natta M, Behling C, Contos MJ, Cummings OW, Ferrell LD, Liu YC, Torbenson MS, Unalp-Arida A, et al: Design and validation of a histological scoring system for nonalcoholic fatty liver disease. Hepatology 41: 1313-1321, 2005.
20. Livak KJ and Schmittgen TD: Analysis of relative gene expression data using real-time quantitative PCR and the 2(-Delta Delta C(T)) method. Methods 25: 402-408, 2001.
21. Gomez G and Sitkovsky MV: Differential requirement for A2a and A3 adenosine receptors for the protective effect of inosine in vivo. Blood 102: 4472-4478, 2003.

22. Yoda-Murakami M, Taniguchi M, Takahashi K, Kawamata S, Saito K, Choi-Miura NH and Tomita M: Change in expression of GBP28/adiponectin in carbon tetrachloride-administrated mouse liver. Biochem Biophys Res Commun 285: 372-377, 2001.
23. Madi L, Bar-Yehuda S, Barer F, Ardon E, Ochaion A and Fishman P: A3 adenosine receptor activation in melanoma cells: Association between receptor fate and tumor growth inhibition. J Biol Chem 278: 42121-42130, 2003.
24. Ge WS, Wang YJ, Wu JX, Fan JG, Chen YW and Zhu L: β-catenin is overexpressed in hepatic fibrosis and blockage of Wnt/β-catenin signaling inhibits hepatic stellate cell activation. Mol Med Rep 9: 2145-2151, 2014.
25. Wang JN, Li L, Li LY, Yan Q, Li J and Xu T: Emerging role and therapeutic implication of Wnt signaling pathway in liver fibrosis. Gene 674: 57-69, 2018.
26. Núñez KG, Gonzalez-Rosario J, Thevenot PT and Cohen AJ: Cyclin D1 in the liver: Role of noncanonical signaling in liver steatosis and hormone regulation. Ochsner J 17: 56-65, 2017.
27. Udomsinprasert W, Honsawek S and Poovorawan Y: Adiponectin as a novel biomarker for liver fibrosis. World J Hepatol 10: 708-718, 2018.
28. Chen GJ, Harvey BK, Shen H, Chou J, Victor A and Wang Y: Activation of adenosine A3 receptors reduces ischemic brain injury in rodents. J Neurosci Res 84: 1848-1855, 2006.
29. Cross HR, Murphy E, Black RG, Auchampach J and Steenbergen C: Overexpression of A(3) adenosine receptors decreases heart rate, preserves energetics, and protects ischemic hearts. Am J Physiol Heart Circ Physiol 283: H1562-H1568, 2002.